2023 年 3 月　　岩　矿　测　试　　Vol. 42, No. 2
March 2023　　ROCK AND MINERAL ANALYSIS　　346-360

尚文郁, 孙青, 谢曼曼,等. 中国东北干旱-半干旱地区湖泊沉积物木质素酚类化合物特征及其气候指示意义[J]. 岩矿测试, 2023,42(2):346-360. doi: 10.15898/j.cnki.11-2131/td.202208210153.

SHANG Wenyu, SUN Qing, XIE Manman, et al. Characteristics of Lignin-derived Phenolic Compounds in Arid Lake, Northeastern China and Climatic Implications[J]. Rock and Mineral Analysis, 2023, 42(2): 346-360. doi: 10.15898/j.cnki.11-2131/td.202208210153.

# 中国东北干旱-半干旱地区湖泊沉积物木质素酚类化合物特征及其气候指示意义

尚文郁, 孙青*, 谢曼曼, 战楠
(自然资源部生态地球化学重点实验室, 国家地质实验测试中心, 北京 100037)

**摘要:** 木质素广泛分布于维管植物,经分解生成的酚类化合物可示踪有机质来源、评估木质素降解程度,进而用于反演古环境与古气候变化。采用合适的分析方法有效地分解木质素是推断母源植物类型、降解程度的技术基础,常规方法是木质素经碱(或酸)解后,利用气相色谱-质谱法(GC-MS)分析酚类单体化合物,但分解、提取过程复杂、易引入杂质。热裂解技术可在高温下快速分解有机质,裂解产物可通过 GC-MS 进行在线分析,具有用样量少、有机质提取比例高、重现性好、操作便捷的特点。本文选择地处亚洲夏季风影响区域的边缘的内蒙伊和沙日乌苏湖,采用热裂解 GC-MS(Py-GC/MS)技术,对湖泊沉积物进行裂解分析,在对裂解温度(450℃、550℃和 650℃)进行了优化的基础上,识别了 21 种酚类化合物,包括:4-甲基苯酚、2-乙基苯酚等 9 种烷基酚类(PHs),4-乙基-2-甲氧基苯酚、4-乙烯基-2,6-二甲氧基苯酚等 9 种烷基酚类(PHs)和 12 种甲氧基酚类(LGs)。结合沉积岩心样品 AMS $^{14}$C 年龄的分析结果,6.7ka 以来沉积物中酚类化合物总量、PHs 和 LGs 的变化趋势总体一致,呈现出 6.7~4.0ka 相对含量较高、4.0ka 以来相对含量较低的特征。不同于 PHs 中邻(*o*-)-PHs、间(*m*-)-PHs、对(*p*-)-PHs 的变化趋势与总量一致;但不同取代特征的 LGs 相对含量变化趋势存在差异, *p*-LGs 在 5.4ka 前后就出现含量显著下降,3.8ka 以来维持较低水平。根据微生物对木质素的“去甲基/去甲氧基”氧化反应途径,对位取代酚类化合物比值(*p*-PHs/*p*-LGs)可作为陆生高等植物降解指标,该值越大微生物降解作用越强。将 *p*-PHs/*p*-LGs 指标应用于伊和沙日乌苏沉积物样品结果显示,6.7ka 以来 *p*-PHs/*p*-LGs 与正构烷烃单体碳同位素 $\delta^{13}\mathrm{C}_{27\sim33}$ 变化趋势一致($R=-0.77$),间接地指示了有效降水变化。即 6.7ka 以来气候整体转湿,区内陆生高等植物占据优势,充足的水分和有机质为微生物提供了适宜的生存环境和相对稳定的营养来源,降解作用整体呈增强趋势;6.3~5.5ka 和 4.1~3.6ka 期间有效湿度降低,微生物对木质素的降解作用相对减弱。*p*-PHs/*p*-LGs 指标对应了呼伦贝尔地区湿度变化特征,揭示了干旱-半干旱地区微生物降解与有效湿度变化的相关性,为探讨陆地生态系统对东亚季风北部边缘区气候变化的响应提供科学依据。

**关键词:** 热裂解-气相色谱-质谱法; 伊和沙日乌苏湖; 木质素酚类单体化合物; 微生物降解; 古气候

---

**收稿日期:** 2022-08-21; **修回日期:** 2022-09-29; **接受日期:** 2022-11-01

**基金项目:** 国家自然科学基金青年基金项目“基于红外光谱的金川泥炭中有机碳、腐殖酸、木质素等古气候替代指标快速分析方法及在古气候研究中的应用”(41402325); 国家自然科学基金面上项目“末次冰盛期以来中—缅热带玛珥湖古温度重建”(41877301); 中央级科研院所基本业务经费项目“湖泊沉积物中记录区域健康风险评价的生态环境指标 ACL 的研究”(CSJ-2021-09)

**第一作者:** 尚文郁,博士研究生,助理研究员,从事环境地球化学及气候替代指标研究。E-mail: shangwenyu@cags.ac.cn。

**通信作者:** 孙青,博士,研究员,从事全球变化研究工作。E-mail: sunqing1616@yahoo.com。

**要点:**

(1) Py-GC/MS 分析伊和沙日乌苏湖泊沉积物中木质素酚类化合物的适宜裂解温度为 650℃。

(2) 沉积物中 PHs 和 LGs 分布特征差异主要来自微生物的“去甲基/去甲氧基”降解反应,降解指标 $p$-PHs/$p$-LGs 数值越大,木质素经历降解的程度越高。

(3) 6.7ka 以来伊和沙日乌苏湖 $p$-PHs/$p$-LGs 与正构烷烃单体碳同位素 $\delta^{13}C_{27\sim33}$ 变化趋势一致,可能间接地指示了该区域(干旱-半干旱地区)有效湿度变化。

**中图分类号:** O657.63; P512.2　　　**文献标识码:** A

木质素是一种三维网状高分子聚合物,分子量从几百到几万,是组成裸子、被子植物茎结构的重要大分子有机化合物,广泛地存在于木本、草本等陆生维管植物细胞壁结构中[1]。木质素基本结构单元为苯丙烷,苯环及其侧基存在大量官能团(如羟基、甲氧基、羰基等),经分解后可生成一系列具有不同官能团的酚类化合物,可指示有机质来源和降解程度,在有机质来源解析及示踪、古气候古环境重建等研究领域得到了广泛应用[2-6]。

选择合适方法对木质素进行高效分解是开展应用研究的基础。常用方法是通过 CuO 在高温下进行碱(或酸)解,生成一系列具有酚羟基和甲氧基结构的酚醛、酚酮和酚酸单体化合物,在衍生化后进行气相色谱-质谱(GC-MS)分析[7-9],实验流程复杂、耗时,易损失目标化合物或引入杂质,可能影响植被种类等自然信息的客观解译。热裂解 GC-MS(Py-GC/MS)技术通过瞬时高温使大分子化合物化学键发生断裂,生成一系列小分子化合物,替代了传统化学提取的预处理方法,实现了对不易气化的复杂有机质的在线分析。该技术具有用样量少、有机质提取比例高、重现性好、操作便捷的特点。Meuzelaar 等[10]利用 Py-GC/MS 技术开展了土壤中腐植酸裂解特征研究,展示了其在土壤有机质特征识别、天然大分子结构表征方面的优势。Bracewell 等对湖泊、泥炭、河口三角洲及沿海大陆架等多类型沉积物开展了热裂解分析,发现木质素高温裂解产物与传统 CuO 氧化分解结果相近[11-18],酚类化合物的分布特征可指示植被类型和有机质降解特征[19-22]。近年来国内外研究多集中于有机质含量较高的样品,有机质整体指纹特征及其生态效应成为研究热点,对于裂解产物中特定组分(如酚类化合物等)仍需开展不同类型样品的分析方法优化、环境指示意义应用及对比研究。

本文利用 Py-GC/MS 对中国东北半干旱地区伊和沙日乌苏湖泊沉积物中木质素酚类化合物进行识别,讨论了酚类化合物的分布特征,结合传统气候指标探讨了木质素酚类化合物与区域气候的相关性,为拓展生物标志物指标体系、揭示陆地生态系统对全球变化的响应提供有效手段。

## 1　研究区概况

伊和沙日乌苏湖位于内蒙古呼伦贝尔草原西北部沙地西部(图 1),是形成于风蚀盆地内的以晚更新世—早全新世沉积物($Q_p^{3fl}$-$Q_h^1$)为基底的风蚀

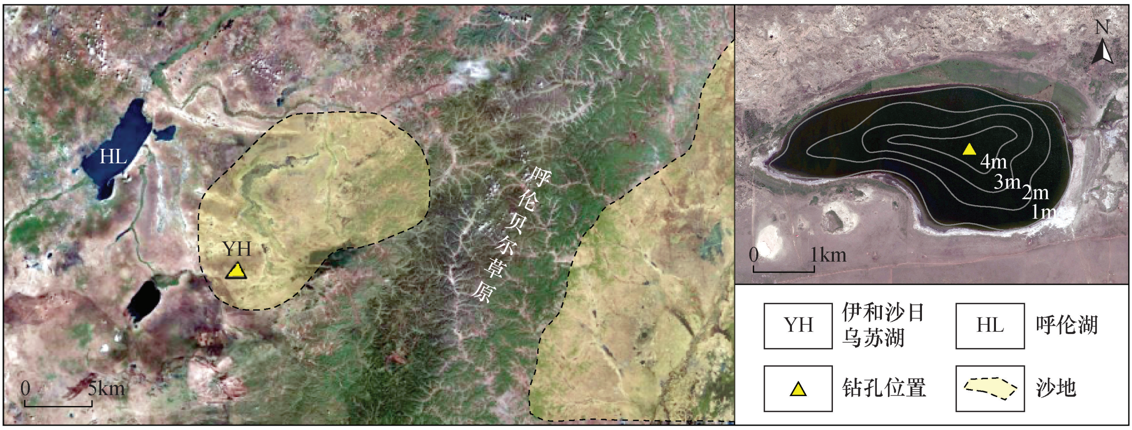

**图 1　内蒙古伊和沙日乌苏湖与采样点位图**

Fig. 1　Location and coring site of Yiheshariwusu Lake in Inner Mongolia.

湖。湖泊为封闭式咸水湖，水源主要来自大气降水及汇水区域的地下水补给。区内植被由多年生草本为主，如大针茅（*Stipa grandis*）、中国羊草（*Leymus chinensis*）、差不嘎蒿（*Artemisia halodendron*）、冷蒿（*Artemisia frigida Willd.*）及沙柳（*Salix gordejevii Chang et SkV.*）等，具有典型的草原植被特征[23]。

## 2 实验部分

### 2.1 样品采集与前处理

在湖泊中心利用无扰动重力钻进行钻探，得到6.7ka以来沉积岩心样品（编号YH-2017），AMS $^{14}$C等相关测年数据详见Xie等[23]对同钻孔样品的研究。本研究中选择了不同深度的样品31个（YH-1至YH-31），样品类型涵盖黏土质粉砂、粉砂质黏土及砂质黏土。

利用冻干机去除样品中的水分后，去掉肉眼可见石块等杂质，结合酚类化合物响应强度对称样量进行调整，准确称量3~5mg样品于专用石英管内，两端放置适量石英棉，以防止样品飞散且助于吸附无机盐等难以气化物质，以待后续热裂解分析[24-25]。

### 2.2 实验仪器与条件参数

样品通过居里点裂解仪（CDS 5200型，美国CDS公司）在无氧条件下进行热解。裂解气在线传输，经气相色谱进样口达到气相色谱-离子阱质谱仪（450GC/240MS，美国Varian公司）。相关气相色谱、质谱分析条件参考了Schellekens等学者对富有机质土壤及湖泊沉积物样品的分析方法[26-35]，并针对低有机质沉积物样品进行了方法改进[25,36]。

气相色谱-质谱分析条件为：进样口温度270℃（高纯He，纯度99.999%），恒流模式柱流速1mL/min。DB-1MS毛细管色谱柱（60m×0.25mm×0.25μm，美国Agilent J&W公司）。炉箱升温程序共91min，初温40℃，升温速率4℃/min，终温320℃（保持18min）。质谱部分：采用电子轰击离子源内源模式（Internal EI），电子能量70eV；离子源温度220℃，歧管温度40℃，传输线温度280℃；采用全扫描模式，扫描范围40~450amu。

### 2.3 数据处理与质量控制

采集的原始数据利用MS Workstation（Version 6.9.3）离线处理，利用扣除背景后目标化合物的峰面积与总峰面积的比值得到酚类化合物的相对含量。在实验过程中，通过插入空白样和重复样确保测试数据的可靠性，计算3倍信噪比（$S/N$）得到检出限（$<1.49\times10^{-5}$），分析结果均在检出限以上，5次平行实验目标化合物相对含量测量结果的RSD<5%，方法重现性良好。

## 3 结果与讨论

### 3.1 酚类化合物的识别

裂解产物中酚类化合物根据官能团类型主要分为两大类：烷基酚类化合物（Alkyl-phenol Compounds，PHs）和甲氧基酚类化合物（Lignin Monomer Compounds，LGs），各化合物再根据苯环结构上的取代基位置区分为邻（*o*-）、间（*m*-）、对（*p*-）化合物，即2（或6）-取代、3（或5）-取代、4-取代的酚类化合物。根据质谱裂解规律[37]，含有苯环结构的酚类化合物分子离子峰很强，可以推断目标化合物分子量和分子式，结合保留时间、特征碎片离子峰及其丰度大小可以判断取代基的位置和类型。经质谱分析，参考NIST标准数据库（NIST2008及NIST Chemistry WebBook）和质谱裂解相关文献，鉴定出酚类化合物21种，其中包括烷基酚类化合物（PHs）9种、甲氧基酚类化合物（LGs）12种（表1）。代表性化合物的选择离子色谱图及质谱图详见图2。

表1 伊和沙日乌苏湖沉积物裂解产物中酚类化合物

Table 1 Pyrolytic phenolic compounds in sediment of Yiheshariwusu Lake

| 代号 | 化合物名称 | 保留时间（min） | 化学式 | 分子量 | 特征离子（*m/z*） |
|---|---|---|---|---|---|
| PH1 | 苯酚<br>Phenol | 20.14 | $C_6H_6O$ | 94 | 94 |
| PH2 | 2-甲基苯酚<br>2-Methylphenol | 23.02 | $C_7H_8O$ | 108 | 107，108 |
| PH3 | 苯乙酮<br>Acetophenone | 23.22 | $C_8H_8O$ | 120 | 105，77 |
| PH4 | 4-甲基苯<br>4-Methylphenol | 23.87 | $C_7H_8O$ | 108 | 107，108 |
| PH5 | 2-乙基苯酚<br>2-Ethylphenol | 26.26 | $C_8H_{10}O$ | 122 | 107，122 |
| PH6 | 3-乙基苯酚<br>3-Ethylphenol | 26.67 | $C_8H_{10}O$ | 122 | 107，122 |
| PH7 | 4-乙基苯酚<br>4-Ethylphenol | 27.36 | $C_8H_{10}O$ | 122 | 107，122 |
| PH8 | 2-乙基-6-甲基苯酚<br>2-Ethyl-6-methylphenol | 29.59 | $C_9H_{12}O$ | 136 | 121，136 |
| PH9 | 2-乙基-5-甲基苯酚<br>2-Ethyl-5-methylphenol | 29.97 | $C_9H_{12}O$ | 136 | 121，136 |
| LG1 | 2-甲氧基苯酚<br>2-Methoxyphenol（Guaiacol） | 23.22 | $C_7H_8O_2$ | 124 | 109，124 |
| LG2 | 4-甲氧基苯酚<br>Methoxyphenol | 24.24 | $C_7H_8O_2$ | 124 | 109，124 |

**(续表1)**

| 代号 | 化合物名称 | 保留时间(min) | 化学式 | 分子量 | 特征离子($m/z$) |
|---|---|---|---|---|---|
| LG3 | 5-甲基-2-甲氧基苯酚<br>Methoxy-5-methylphenol<br>(5-Methylguaiacol) | 28.07 | $C_8H_{10}O_2$ | 138 | 123, 138 |
| LG4 | 4-乙基-2-甲氧基苯酚<br>4-Ethyl-2-methoxyphenol<br>(4-Ethylguaiacol) | 31.42 | $C_9H_{12}O_2$ | 152 | 137, 152 |
| LG5 | 4-乙烯基-2-甲氧基苯酚<br>4-Vinyl-2-methoxyphenol<br>(4-Vinylguaiacol) | 32.54 | $C_9H_{10}O_2$ | 150 | 135, 150 |
| LG6 | 2,6-二甲氧基苯酚<br>2,6-dimethoxyphenol (Syringol) | 33.46 | $C_8H_{10}O_3$ | 154 | 154, 139 |
| LG7 | 4-(2-丙烯基)-2-甲氧基苯酚<br>4-(2-Propenyl)-2-methoxyphenol<br>(Eugenol) | 37.06 | $C_{10}H_{12}O_2$ | 164 | 164, 149 |
| LG8 | 4-乙酰基-2-甲氧基苯酚<br>4-Acetyl-2-methoxyphenol (4-Acetylguaiacol) | 37.85 | $C_9H_{10}O_3$ | 166 | 151, 166 |
| LG9 | 4-乙基-2,6-二甲氧基苯酚<br>4-Ethyl-2,6-dimethoxyphenol<br>(4-Ethylsyringol) | 39.19 | $C_{10}H_{14}O_3$ | 182 | 167, 182 |
| LG10 | 4-乙烯基-2,6-二甲氧基苯酚<br>4-Vinyl-2,6-dimethoxyphenol (4-Vinylsyringol) | 40.28 | $C_{10}H_{12}O_3$ | 180 | 165, 180 |
| LG11 | 4-羟基-3,5-二甲氧基苯甲醛<br>4-Hydroxy-3,5-dimethoxybenzaldehyde<br>(syringaldehyde) | 43.06 | $C_9H_{10}O_4$ | 182 | 182, 181 |
| LG12 | 4-(1-丙烯基)-2,6-二甲氧基苯酚<br>4-(1-Propenyl)-2,6-dimethoxyphenol<br>(4-Propenylsyringol) | 44.21 | $C_{11}H_{14}O_3$ | 194 | 194, 91 |

烷基酚(以乙基苯酚为例)：主要碎片为 $m/z$ 122、107和77,利用特征碎片作为选择离子提取乙基苯酚,根据保留时间和 $m/z$ 122、$m/z$ 77丰度比值,依次确定为邻、间、对-乙基苯酚,保留时间分别为26.26min、26.67min和27.36min。其中,对乙基苯酚的质谱裂解途径为分子离子[$C_8H_{10}O$]($m/z$ 122)失去甲基自由基生成基峰[$C_7H_7O$]离子($m/z$ 107),再经重排、失去[CO]离子、2个氢原子后生成[$C_6H_5$]$^-$离子($m/z$ 77)。

甲氧基酚(以甲氧基苯酚为例)：主要碎片为 $m/z$ 124、109和81,利用特征碎片作为选择离子提取甲氧基苯酚,根据保留时间和 $m/z$ 124和 $m/z$ 81丰度比值,依次确定为邻甲氧基苯酚和对甲氧基苯酚,保留时间分别为23.22min和24.24min。其中,邻甲氧基苯酚的质谱裂解途径为分子离子[$C_7H_8O_2$]($m/z$ 124)失去甲基自由基生成基峰[$C_6H_5O_2$]离子($m/z$ 109),再失去[CO]离子后生成[$C_5H_5O$]离子($m/z$ 81)。

## 3.2　Py-GC/MS分析中裂解温度的优化

裂解温度可能是影响裂解产物特征和Py-GC/MS分析结果的主要因素[38-39]。首先,不同化学键的键能不同,裂解温度对应的裂解能量高于某化学键键能时,化学键发生断裂形成分子量更小的化合物[28],断裂位置不同,产物特征不同;其次,根据植物、湖泊沉积物、泥炭、表层土壤分析结果,有机质裂解存在基体效应,不同裂解温度下产物分布特征存在差异[22,31,40-45]。此外,不同型号热裂解装置的样品舱设计和热传输机制存在差异,最高可达150℃[46-47]。本文利用配备铂丝探头的居里点裂解仪,选择不同基质样品(黏土质和砂土质)11件,分别在450℃、550℃和650℃下讨论不同裂解温度对裂解产物分布特征的影响,得到了分析酚类化合物的适宜条件。

### 3.2.1　裂解温度对酚类化合物总量的影响

伊和沙日乌苏湖泊沉积物的裂解产物可分为具有—$CH_2$骨架的直链脂肪族类脂化合物、含氮化合物、多糖类衍生物、芳香烃类化合物和木质素酚类化合物5大类。通过对比不同裂解温度下裂解产物及其相对含量发现,随着裂解温度升高,木质素酚类化合物的相对含量显著增加。450℃下裂解产物中酚类化合物相对含量仅为3.77%,在5类化合物中占比最低(图3a);550℃下木质素、蛋白质等天然大分子的侧基发生断裂,产生了一系列具有芳香结构和含氮基团的小分子,裂解产物中酚类化合物的相对含量提高到8.44%,同时伴随着芳香烃类和含氮化合物相对含量的升高其相对含量分别增加至26.75%和39.98%(图3b);650℃时连接木质素骨架结构苯丙烷结构单元的醚键(C—O—C)进一步断裂,裂解产物中酚类化合物相对含量达到最高(16.46%),芳香烃类和脂肪族类脂化合物的占比提高,分别增加至30.73%和25.33%(图3c),未发现随裂解温度升高引发缩合、环化反应,而造成裂解产物中的目标化合物被消耗的现象。

### 3.2.2　裂解温度对目标化合物响应强度的影响

裂解温度为650℃时,多数样品的酚类化合物达到了最高离子强度响应,不易气化的天然大分子化合物在高温下逐步裂解为小分子的酚类化合物离子碎片,进入色谱系统的酚类化合物通量升高,气相色谱响应逐渐增强。同时,单位峰面积、色谱峰型和

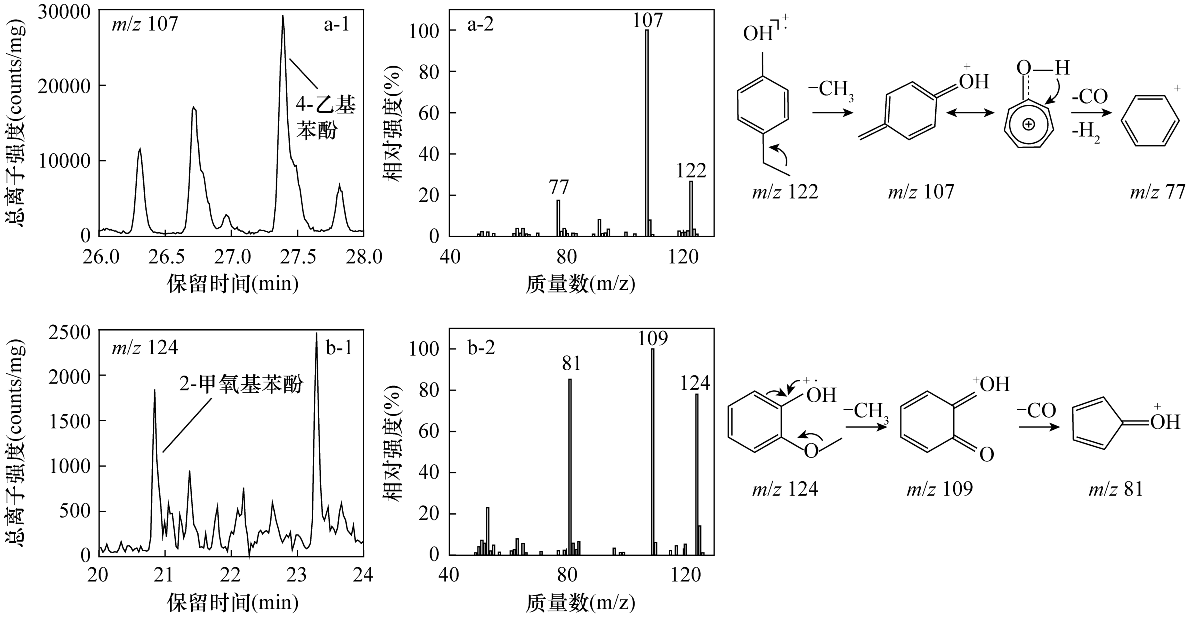

a-1、a-2—*m/z* 107 选择离子色谱图及对乙基苯酚质谱图及裂解特征;

b-1、b-2—*m/z* 124 选择离子色谱图及邻甲氧基苯酚质谱图及裂解特征。

**图 2　样品中不同类型酚类化合物选择离子色谱图及质谱裂解特征**

Fig. 2　Selective ion chromatogram, mass spectra and fragmentation characteristics of phenolic compounds.

a-1 and a-2—*m/z* 107 selective ion chromatogram, mass spectra and fragmentation characteristics of 4-ethylphenol;

b-1 and b-2—*m/z* 124 selective ion chromatogram, mass spectra and fragmentation characteristics of 2-methoxyphenol.

信噪比三方面均有提升,提高了酚类化合物识别、分析的准确性。以 4-甲基苯酚为例,随着裂解温度升高,在 650℃时目标化合物峰型对称且尖锐,峰面积最高 $1.18\times10^6$counts · min/mg,信噪比最佳($S/N=68$)(图 3d);以 4-乙烯基-2-甲氧基苯酚(4-乙烯基愈创木酚)为例,在不同裂解温度下峰高相近,随温度升高色谱流出信号半峰宽呈减小的趋势,在 650℃时色谱信号峰型较好,有利于对目标化合物峰面积的准确计算。

根据前期开展同一钻孔样品的热裂解分析方法研究结果,分析脂肪族类脂(结合态)的适宜裂解温度为 550℃[36],但木质素的高分子、三维网状结构更稳定,断裂 C—O 键和 C—C 键需要的能量更高,对应分析酚类化合物的裂解温度相应升高,如 Kaal 等分析泥炭、海洋沉积物及高寒草原土壤中木质素酚类化合物的裂解温度均在 650℃及以上[20,29,31,48-49]。同时考虑到碳酸盐等无机矿物可促进有机质化学键的断裂,降低有机质热解活化能[22,50-52],当样品中无机碳含量较高时,裂解所需温度降低,温度过高时可能引起副反应。伊和沙日乌苏湖湖水的矿化度高,湖泊沉积物样品无机碳含量高,裂解有机质所需能量不宜过高,以避免副产物的增加。因此,将 650℃作为适宜裂解温度应用于对伊和沙日乌苏沉积物样品的分析。

### 3.3　湖泊沉积物中酚类化合物的分布特征

利用上述裂解温度应用于总计 31 个伊和沙日乌苏湖泊沉积物样品的分析,裂解产物中均有酚类化合物检出,总酚类化合物在总裂解产物中平均占比为 40.84%。酚类化合物以烷基酚(PHs)为主,甲氧基酚(LGs)占比较低,两类物质在酚类化合物总量中平均占比分别为 89.3%和 3.63%。6.7ka 以来各酚类化合物的变化趋势总体一致,表现为 6.7~4.0ka 期间酚类化合物相对含量较高、4.0ka 以来较低的特征(图 4)。

PHs 在总裂解产物中平均占比为 37.22%,邻($o$-)、间($m$-)、对($p$-)位取代的相对含量相近(图 4 中 b~e)。PHs 总量在 6.7~4.0ka 期间相对含量较高,在 4.0ka 前后显著降低(降幅达到 75.46%),4.0ka 以来维持较低水平并经历多次波动。$o$-PHs、$m$-PHs、$p$-PHs 的变化趋势与总量一致。LGs 在总裂解产物中平均占比为 3.62%,其中$p$-LGs 较低,平均占比为 1.04%(图 4 中 f~h)。LGs 与 PHs 变化趋势相近,在 5.7~5.4ka、2.8ka、1.8~1.4ka 有细节上差异。$m$-LGs 具有与 LGs 一致的变化趋势,$p$-LGs 在 5.4ka 前后就出现含量显著下降,3.8ka 以来维持较低水平(平均占比为 0.29%)。

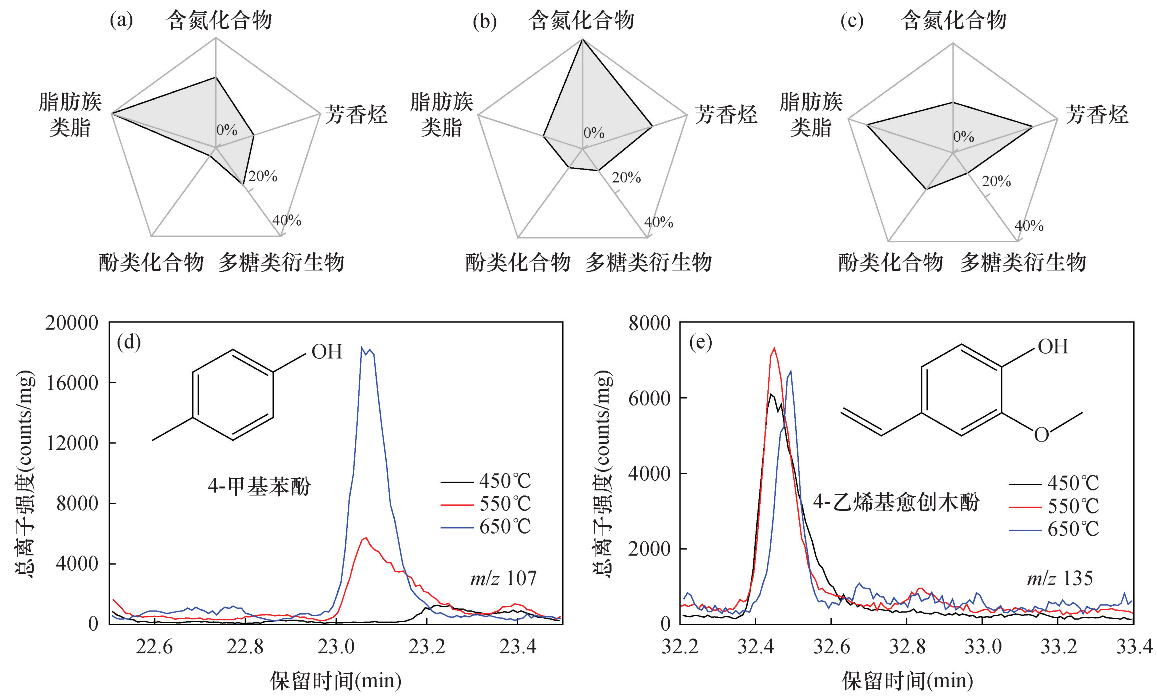

a—裂解温度为 450℃；b—裂解温度为 550℃；c—裂解温度为 650℃；d—选择离子 $m/z=107$ 色谱图；e—选择离子 $m/z=135$ 色谱图。

**图 3　不同裂解温度下产物相对含量分布及目标化合物色谱响应对比图**

Fig. 3　Distribution of pyrolytic compounds (five categories are N-compounds, aromatics, polysaccharide derivatives, phenols and aliphatic compounds clockwise) and chromatographic responses of typical phenolic compounds under different pyrolytic temperatures. a—450℃ of pyrolytic temperature; b—550℃ of pyrolytic temperature; c—650℃ of pyrolytic temperature; d—selective ion chromatogram of $m/z$ 107; e—selective ion chromatogram of $m/z=135$.

结合沉积物岩心特征,酚类化合物总量及 PHs 相对含量在 4.0ka 前后显著降低,可能原因是在 185~175cm(对应年龄 4.0~3.8ka)沉积岩性发生变化,由 4.0ka 之前的砂土变为粒径较小的粉质黏土,分子量较小的化合物得以在沉积物中保存下来,裂解产物中直链脂肪类脂(如正构烷烃、正构烯烃)及芳香烃类化合物的相对含量增加。

## 3.4　酚类化合物的环境指示意义

在具有各类结构特征的木质素裂解酚类化合物中,对位取代烷基酚类化合物(*p*-PHs)和甲氧基酚类化合物(LGs)反映了木质素来源植被类型。Saiz-Jimenez 等通过对不同标型木质素进行裂解实验发现,木本植物以 LGs 为主,其中 *p*-PHs 含量极低;草本植物中 *p*-PHs 含量较高,与 LGs 含量相近[8]。同时,微生物对有机质的降解作用不可忽视。Dittmar 等发现棕腐菌等真菌对木质素的“去甲基/去甲氧基”降解作用可反映酚类化合物中 *p*-PHs 和 LGs 的分布特征,降解作用越强,对烷基酚与甲氧基酚的比值 *p*-PHs/LGs 越大[53-57],因此可用于指示湖泊、河口、滨海沉积物中微生物作用对木质素的降解程度[54,58-60]。

### 3.4.1　酚类化合物降解指标的建立

根据伊和沙日乌苏湖泊沉积物中 *p*-PHs 和 LGs 变化特征(图 4 中 c,f),较高的 *p*-PHs 相对含量指示木质素来源以草本植物为主,但 *p*-PHs 与 LGs 相对含量平均值相差 8.92 倍,指示了微生物对有机质的显著降解。自然界中参与降解木质素的细菌、真菌、放线菌等主要通过胞外木质素降解酶(如木质素过氧化物酶、锰依赖过氧化物酶和漆酶等)的参与,优先断裂木质素结构单元之间具有对位特征的 β-O-4 醚键,生成一系列对位取代甲氧基酚类化合物,进而通过“去甲基/去甲氧基”氧化反应途径生成具有对位特征的烷基酚类化合物[61-64]。因此,对位取代酚类化合物比值(*p*-PHs/*p*-LGs)可反映木质素的降解程度,在本文中的计算公式为:

$$p\text{-PHs}/p\text{-LGs}=\frac{\mathrm{PH4+PH7}}{\mathrm{LG4+LG5+LG7+LG8+LG9+LG10+LG12}}$$

式中:PH4、PH7 表示本文中识别出的具有羟基对位取代结构特征的烷基酚类化合物;LG4、LG5、LG7、LG8、LG9、LG10、LG12 表示具有羟基对位取代结构特征的甲氧基酚类化合物。

将 *p*-PHs/*p*-LGs 指标应用于解析伊和沙日乌

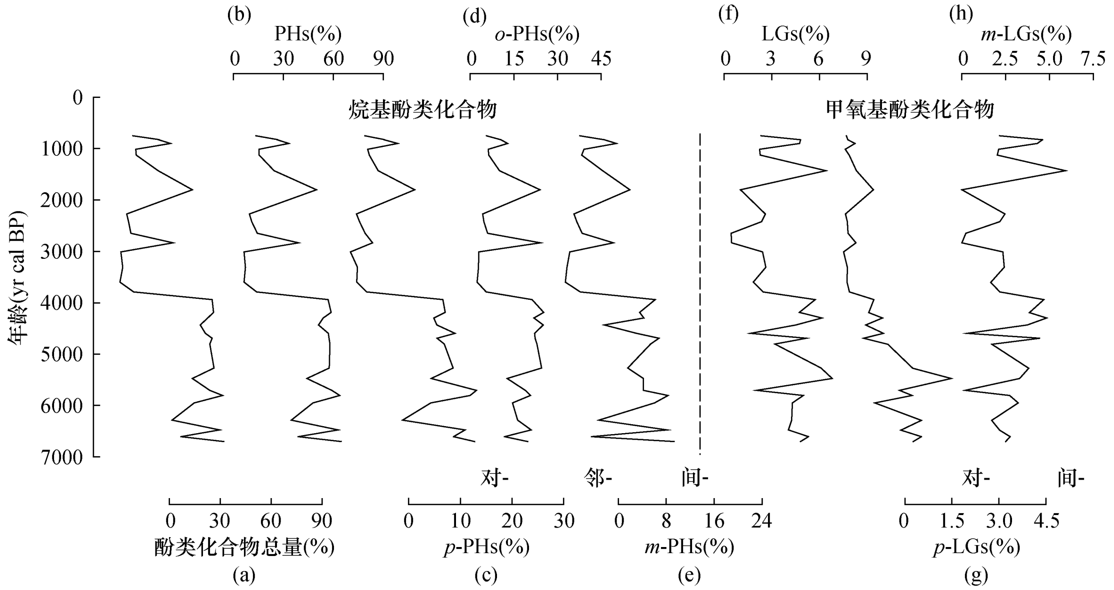

a—酚类化合物在裂解产物中相对含量；b—PHs在裂解产物中相对含量；c、d、e—不同取代PHs占比；
f—LGs在裂解产物中相对含量；g、h—不同取代LGs占比。

**图4　酚类化合物在总裂解产物中的相对含量及分布特征**

Fig. 4　Historical variation of phenolic compounds in pyrolytic compounds. a—Relative concentration of phenolic compounds in pyrolysis products; b—Relative concentration of PHs in pyrolysis products; c, d, e—Proportion of different substituted PHs; f—Relative concentration of LGs in pyrolysis products; g, h—Proportion of different substituted LGs.

苏沉积物31件样品，结果显示$p$-PHs/$p$-LGs平均值为16.41，变化范围为4.36～37.31，指示经历了显著的降解作用。发源于植物叶蜡正构烷烃的传统指标，如平均碳链长度指标(Average Carbon Length, ACL)、$C_{31}/(C_{27}+C_{29}+C_{31})$和碳优势指数(Carbon Preference Index, CPI)可有效地区分植被类型，评价微生物对有机质降解的影响。Xie等报道的伊和沙日乌苏样品同一钻孔结果显示，8.5ka以来$ACL_{23\sim33}$及$C_{31}/(C_{27}+C_{29}+C_{31})$变化不大(图5中a, b)，区内植被类型以典型草原为主，包括草甸草原、稀疏沙地草原等[23]，草本和木本比例无显著变化，$CPI_{23\sim33}$则呈现了从6.7ka以来逐渐降低的趋势(图5c)，与$p$-PHs/$p$-LGs指标变化趋势相一致(图5d)，指示了陆生高等植物来源的有机质为微生物的降解作用提供了充足的碳源。

### 3.4.2　酚类化合物指标的气候指示意义

伊和沙日乌苏湖所在的呼伦贝尔沙地位于亚洲夏季风影响区域的边缘，Xie等发表的同一钻孔沉积物中长链正构烷烃及其单体碳同位素$\delta^{13}C_{27\sim33}$的研究结果显示，区内有效湿度在6.7ka以来呈逐渐增加的趋势，且6.3～5.5ka和4.1～3.6ka期间相对干旱[23]。酚类化合物降解指标$p$-PHs/$p$-LGs与$\delta^{13}C_{27\sim33}$变化趋势一致(图5e)，并呈负相关($n=31$, $R=-0.77$, $p<0.01$)，指示微生物作用增强。已有高纬、干旱地区研究表明，微生物活性和分解速率与降水量的变化相关[65-66]，区内6.7ka以来气候整体转湿，长链正构烷烃相对含量高，指示陆生高等植物占据优势，充足的水分和有机质为微生物提供了适宜的生存环境和相对稳定的营养来源，降解作用呈逐渐增强；相对干旱期时(6.3～5.5ka和4.1～3.6ka)有效湿度降低，微生物对木质素的降解作用减弱。

同区内的呼伦湖是内蒙古第一大湖，研究程度相对较高，岩心总有机碳(TOC)、$\delta^{13}C_{org}$、粒度、孢粉分析结果显示了东亚夏季风对北部边缘区域降水产生显著影响[67-72]。6.3～6.0ka、4.1～3.6ka、1.1～0.9ka呼伦湖沉积物中值粒径占比增加，同期伊和沙日乌苏湖$p$-PHs/$p$-LGs指标降低，对应降解作用减弱，指示了相对干旱的气候；同时，4.2ka前后呼伦湖沉积物近岸粗粒径占比显著增加，沉积物中砂质比例增加，对应了伊和沙日乌苏湖$p$-PHs/$p$-LGs指标和$\delta^{13}C_{27\sim33}$显著变化，指示了中国普遍发生的全新世季风减弱事件[73-75]。湖泊沉积物样品中花粉组合及花粉通量能较好地反映地方和区域植被特征，呼伦湖沉积物中藜科(*Chenopodiaceae*)、禾本科(*Poaceae*)花粉百分含量除4.1～3.6ka降低以外，6.7ka以来整体呈现增加趋势(图5f)[71]，$p$-PHs/

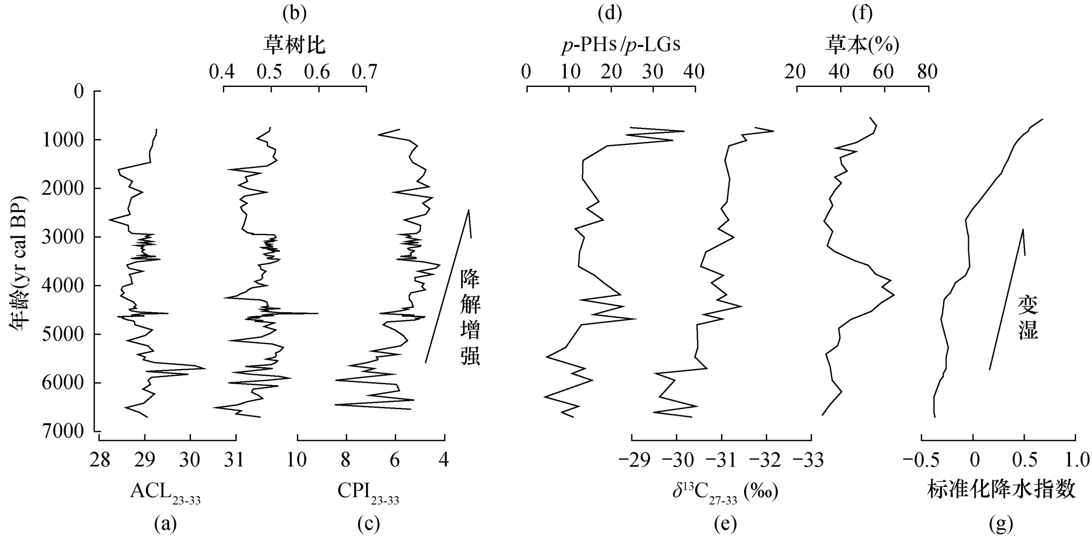

a—正构烷烃平均链长 $ACL_{23\sim33}$[23];b—正构烷烃指示草树比[$C_{31}/(C_{27}+C_{29}+C_{31})$][23];c—正构烷烃碳优势指数 $CPI_{23\sim33}$(逆坐标);d—木质素降解指标(*p*-PHs/*p*-LGs);e—长链正构烷烃单体碳同位素比值;f—呼伦湖草本(禾本科、藜科)孢粉百分含量[71];g—北半球中纬地区标化降水指数[74]。

**图 5　*p*-PHs/*p*-LGs 指标及同区气候指标变化特征**

Fig. 5　Variation of *p*-PHs/*p*-LGs index and climatic records in same region. a—Average chain length $ACL_{23-33}$[23]; b—Ratio of grasses/trees [$C_{31}/(C_{27}+C_{29}+C_{31})$]; c—Carbon predominance index ($CPI_{23-33}$); d—Lignin degradation index (*p*-PHs/*p*-LGs); e—Compound-specific $\delta^{13}C_{27-33}$; f—Herb pollen percentage of Hulun Lake; g—Net precipitation (precipitation minus evapotranspiration) in standard deviation (SD) units in mid-latitude net precipitation.

*p*-LGs 的变化与花粉增加趋势一致,并呈正相关($n=31, R=0.54, p<0.01$),指示草原植被的繁盛,共同体现了呼伦贝尔地区 6.7ka 以来气候转湿。在大尺度上,*p*-PHs/*p*-LGs 和北半球中纬地区(30°N～50°N)标准化降水指数 6.7ka 以来逐渐升高的趋势一致(图 5g)[76],并呈正相关($n=31, R=0.62, p<0.01$),东亚季风北部边缘干旱-半干旱地区有效湿度变化响应了北半球中纬度陆地降水的整体变化。因此,伊和沙日乌苏湖泊沉积物 *p*-PHs/*p*-LGs 可能是有效的干湿指标。

## 4　结论

本文利用 Py-GC/MS 技术对伊和沙日乌苏湖泊沉积物中 21 种木质素酚类化合物进行识别、分析,并根据微生物对木质素的降解途径提出了指示木质素降解程度的指标 *p*-PHs/*p*-LGs。研究表明,伊和沙日乌苏湖泊沉积物中 PHs 和 LGs 分布特征差异主要来自微生物的“去甲基/去甲氧基”降解反应,*p*-PHs/*p*-LGs 可作为陆生高等植物降解指标,该值越大,微生物降解作用越强,6.7ka 以来伊和沙日乌苏湖泊沉积物中木质素受到的降解作用逐渐增加。*p*-PHs/*p*-LGs 与正构烷烃单体碳同位素 $\delta^{13}C_{27\sim33}$ 呈负相关,间接指示了区域有效湿度的变化,识别了区内 6.3～5.5ka 和 4.1～3.6ka 期间相对干旱、6.7ka 以来有效降水整体逐渐增加的干湿变化特征。

考虑到不同生境类型中植被组合可能显著影响木质素酚类化合物组成特征,下一步工作将开展表土及现代植物的热裂解化合物的定性、定量研究,并进行不同气候带的对比,为酚类化合物在全球变化研究中的应用提供基础数据。

# Characteristics of Lignin-derived Phenolic Compounds in Arid Lake, Northeastern China and Climatic Implications

*SHANG Wenyu, SUN Qing**, *XIE Manman, ZHAN Nan*
(Key Laboratory of Eco-Geochemistry, Ministry of Natural Resources, National Research Center for Geoanalysis, Beijing 100037, China)

## HIGHLIGHTS

(1) 650℃ is the suitable pyrolytic temperature for digesting lignin-derived phenolic compounds in the sediments of YihesharIwusu Lake.

(2) The difference in distribution characteristics of PHs and LGs in sediments is mainly due to the "demethylation/demethoxy" degradation reaction of microorganisms. The value of degradation index *p*-PHs/*p*-LGs corresponds to the degree of lignin degradation.

(3) Since 6.7ka, *p*-PHs/*p*-LGs of YihesharIwusu Lake has been consistent with the change trend of carbon isotope $\delta^{13}C_{27-33}$ of *n*-alkane monomer in Xiaolongwan Maar Lake, which may indirectly indicate the change of effective precipitation in this area (arid and semi-arid area).

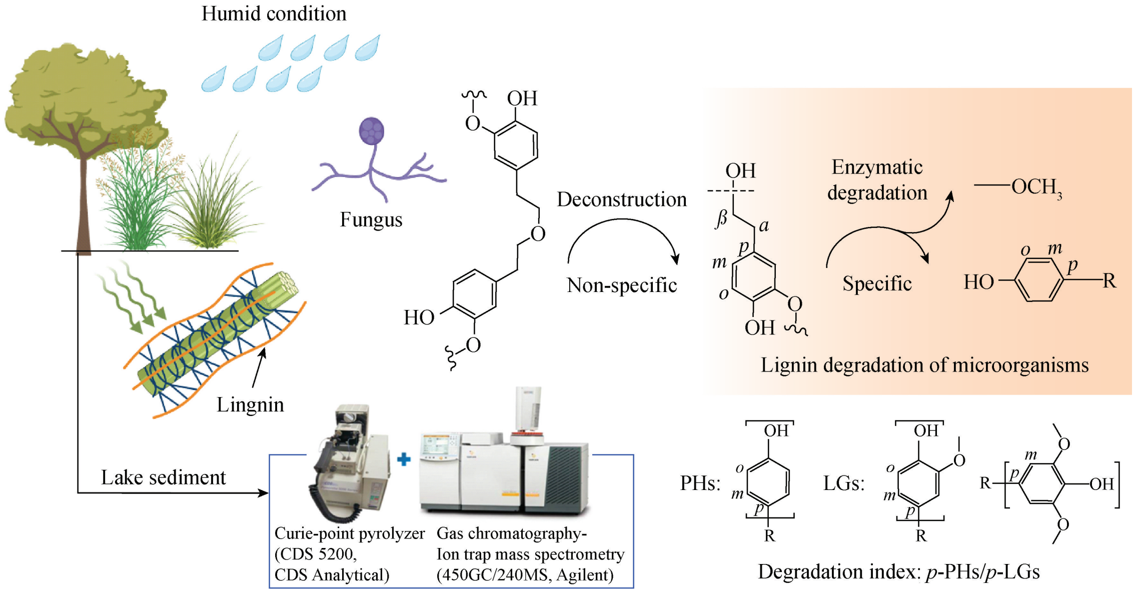

## ABSTRACT

**BACKGROUND:** Lignin is widely distributed in vascular plants, and lignin-derived phenolic compounds generated by decomposition could provide information on the source of organic matter and the degradation degree of lignin. The conventional method for lignin deconstruction is complex and involves lignin hydrolysis *via* alkaline/acid chemical reagents. The analytical technique pyrolysis-gas chromatography-mass spectrometry (Py-GC/MS) breaks the chemical bonds of large molecule compounds by instantaneous high temperature to generate a series of small molecule compounds without introducing pretreatment methods such as chemical extractions, realizing the online analysis of complex organic matter that is not easy to be gasified. This technique is characterized by low sample volume, high organic matter extraction ratio, good reproducibility, and convenient operation. It has been shown that the high-temperature cracking products of peat and lake sediments are similar to the results of traditional CuO oxidative decomposition. The distribution characteristics of phenolic compounds indicate the vegetation type

and organic matter degradation characteristics. However, the optimization of analytical methods, application of environmental indication significance, and comparative studies of different matrix samples are still needed.

**OBJECTIVES**: (1) Investigate suitable analytical methods for decomposing lignin in lake sediment samples and identify pyrolytic phenolic compounds in the sediments of Yihesharіwusu Lake in the northeast semi-arid region of China (Fig. E. 1A, B). (2) Discuss the distribution characteristics of phenolic compounds in the sediments of Yihesharіwusu Lake. (3) Reveal the correlation between pyrolytic lignin phenols and regional climate change in the study area by combining traditional climate proxies, and provide an effective indicator for interpreting the response of terrestrial ecosystems to global climate change.

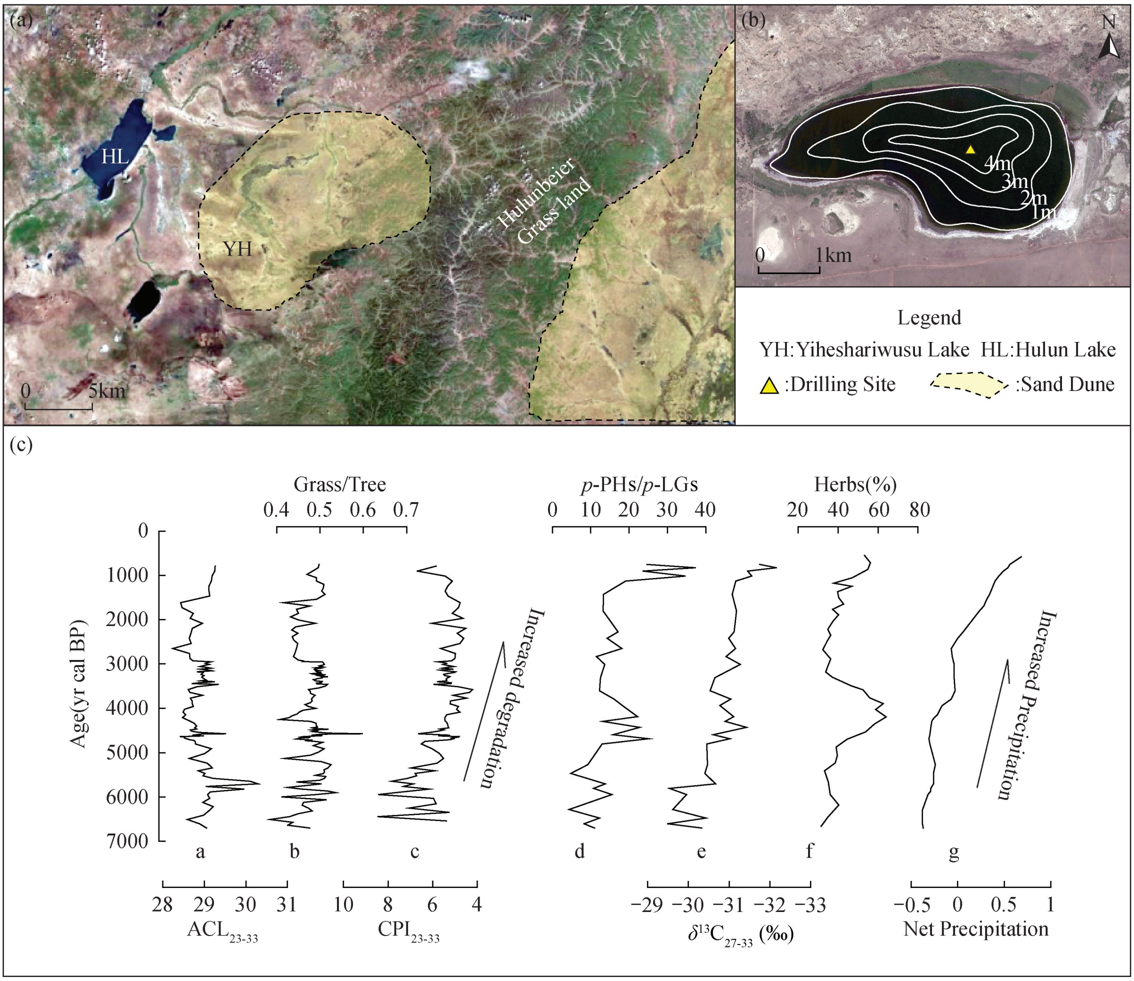

Fig. E. 1　Study site and variation of p − PHs/p − LGs index compared with climatic records in same region. A—Location of Yihesharіwusu Lake, B—Coring site of Yihesharіwusu Lake, C(a)—Average chain length; C(b)—Ratio of grasses/trees; C(c)-Carbon predominance index; C(d) - Lignin degradation index; C(e)—Compound - specific $\delta^{13}C_{27-33}$; C(f)—Herb pollen percentage of Hulun Lake; C(g)—Standardized average mid - latitude (30° N to 50° N) net precipitation.

**METHODS**: (1) Analytical method: An optimized analytical method of Py-GC/MS was established and applied to evaluate lignin-derived phenolic compounds in typical arid lake sediment. Samples were heated to 650℃ for 20s (heating rate 20℃/ms) and pyrolysis products were injected into the gas chromatography (GC) system in split mode, then separated in a nonpolar, low-bleed fused silica column (DB-1MS, 60m, 0.25mm i.d., 0.25μm film thickness, J&W). The GC oven program was set to increase from 40 to 320℃ at a rate of 4℃/min, and left at 320℃ for 18min. With internal electron ionization and ion trapping, the compounds were fragmented and identified in full scan mode (40-450amu). Blank and duplicate samples were analysed for quality control.

(2) Establishment of climatic proxy: Yihesharіwusu was selected as a typical arid lake and pyrolytical phenolic compounds of sediment cores were analysed. Historical variation of phenolic compound combing with radiocarbon dating results were revealed. According to "demethyl/demethoxy" oxidation reaction pathway of microorganisms to lignin, indicator related to degradation degree of lignin was established, and by comparing the indicators with conventional climate proxies previously published in the region, correlations between the indicators and climate features such as effective precipitation can be explored.

**RESULTS**: (1) Py-GC/MS analysis method for phenolic compounds was optimized. Phenolic compounds in the total pyrolytic products of sediments were categorized into 2 groups according to the type of functional group: alkyl-phenols (phenol compounds, PHs) and methoxy-phenols (lignin monomer compounds, LGs), which are further divided into *o*-, *m*- and *p*-compounds according to the position of the substituent on the benzene ring structure. Based on fine characterization of organic matter composition in the sediments of Yihesharіwusu Lake in Inner Mongolia, 21 phenolic compounds were identified and analyzed, including 9 PHs and 12 LGs (Table 1). Pyrolysis temperature is the main factor affecting the results of Py-GC/MS analysis of sediment organic matter fingerprinting. By discussing the effect of different pyrolysis temperatures on the distribution characteristics of the total pyrolytic products at 450℃, 550℃ and 650℃, it was determined that the relative concentration of lignin phenolic compounds increased significantly with increasing pyrolysis temperature. The ether bond (C—O—C) connecting the lignin skeleton structure benzene propane structural unit was further broken as the temperature was increased from 450℃ to 650℃. The relative concentration of phenolic compounds in the pyrolysis compounds reached the highest proportion (16.46%), while the proportion of aromatic hydrocarbons and aliphatic hydrocarbons increased by 3.98% and 10.26%, respectively. The natural macromolecules, which are not easily vaporized, are gradually cleaved into smaller ionic fragments of phenolic compounds under high pyrolysis temperature. As the cleavage temperature increases to 650℃, the flux of phenolic compounds into the chromatographic system increases and the gas chromatographic response is gradually enhanced, with the phenolic compounds reaching the highest ionic intensity response. At the same time, the unit peak area, shape and signal-to-noise ratio were all improved, which improved the accuracy of phenolic compound identification and analysis.

(2) Distribution characteristics of phenolic compounds in Yihesharіwusu Lake were discussed. According to AMS $^{14}$C age data, historical variation of total phenolic compounds, PHs and LGs in lake sediment are generally consistent since 6.7ka, showing the characteristics of high relative concentration of 6.7-4.0ka and low concentration since 4.0ka. The variation characteristics of *o*-PHs, *m*-PHs, and *p*-PHs are consistent with total PHs, yet the change characteristics of *p*-LGs and LGs are different, the relative concentration of *p*-LGs decreased significantly near 5.4ka and remained at a low level since 3.8ka (average relative concentration of 0.29%). Combined with the lithological characteristics of sediment cores, relative concentration of total phenolic compounds and PHs decreased significantly around 4.0ka, probably due to the change of sedimentary lithology from sand to clay with smaller grain sizes during 4.0-3.8ka, where compounds with smaller molecular weights were preserved in the sediments, and the relative concentration of aliphatic hydrocarbons (e.g., *n*-alkanes, *n*-alkenes) and aromatic hydrocarbons significantly increased.

(3) Environmental indication significance of phenolic compounds was studied. According to previous studies of free *n*-alkanes distribution proxies (e.g., $ACL_{23-33}$), higher relative concentration in lake sediments of *p*-PHs indicated major herbaceous source of lignin, however, significant differences in the mean relative concentration of *p*-PHs and LGs indicated significant microbial degradation of organic matter. The mean value of *p*-PHs/*p*-LGs for Yihesharіwusu Lake sediments was 16.41 ($n=31$, range of 4.36-37.31), showing an overall increasing trend since 6.7ka, reflecting a gradual increase in microbial activities. *p*-PHs/*p*-LGs showed a consistent trend and negative correlation with $\delta^{13}C_{27-33}$ ($n=31$, $R=-0.77$, $p<0.01$), meanwhile, variation of *p*-PHs/*p*-LGs positively

correlated with the trend of increasing pollen of Chenopodiaceae and Poaceae in Hulun Lake sediment ($n=31$, $R=0.54$, $p<0.01$), and on a larger scale, $p$-PHs/$p$-LGs are consistent and positively correlated with the gradual increase in the standardized precipitation index since 6.7ka in the northern hemisphere mid-latitudes ($n=31$, $R=0.62$, $p<0.01$) (Fig. E. 1C).

**CONCLUSIONS**: The suitable pyrolysis temperature for Py-GC/MS analysis of phenolic compounds in the sediments of Yihesharіwusu Lake is 650℃. The value of degradation index $p$-PHs/$p$-LGs corresponds to the degree of lignin degradation, and the larger the value, the stronger the microbial degradation. Applying the $p$-PHs/$p$-LGs index to the sediment samples of Yihesharіwusu Lake, the result show that degradation index ($p$-PHs/$p$-LGs) and the carbon isotope of free $n$-alkanes $\delta^{13}C_{27-33}$ has solid correlation since 6.7ka, indirectly indicating the change of effective precipitation, as the climate turned wet generally since 6.7ka, with terrestrial higher plants dominant, humid climate and sufficient organic matter provided a suitable living environment and relatively stable nutrient source for microorganisms, and the degradation generally increased. Since effective precipitation decreased during 6.3-5.5ka and 4.1-3.6ka, the degradation of lignin by microorganisms was relatively weakened. The $p$-PHs/$p$-LGs index corresponds to the characteristics of effective precipitation in the Hulun Buir region, revealing the correlation between microbial degradation and humidity change in arid and semi-arid regions. These findings provide a scientific basis for exploring the response of terrestrial ecosystems to climate change in the northern marginal region of the East Asian monsoon.

**KEY WORDS**: pyrolysis-gas chromatography-mass spectrometry (Py-GC/MS); Yihesharіwusu Lake; lignin-derived phenolic compounds; microbial degradation; paleoclimate

## 参考文献

[1] Vanholme R, Demedts B, Morreel K, et al. Lignin biosynthesis and structure[J]. Plant Physiology, 2010, 153(3):895-905.

[2] Mitra S, Bianchi T S, Guo L, et al. Terrestrially derived dissolved organic matter in the chesapeake bay and the Middle Atlantic Bight[J]. Geochimica et Cosmochimica Acta, 2000, 64(20):3547-3557.

[3] Jex C N, Pate G H, Blyth A J, et al. Lignin biogeochemistry: From modern processes to Quaternary archives[J]. Quaternary Science Reviews, 2014, 87:46-59.

[4] Ward N D, Krusche A V, Sawakuchi H O, et al. The compositional evolution of dissolved and particulate organic matter along the lower Amazon River—Óbidos to the ocean[J]. Marine Chemistry, 2015, 177:244-256.

[5] 冯晓娟,王依云,刘婷,等. 生物标志物及其在生态系统研究中的应用[J]. 植物生态学报, 2020, 44(4):384-394.
Feng X J, Wang Y Y, Liu T, et al. Biomarkers and their applications in ecosystem research[J]. Chinese Journal of Plant Ecology, 2020, 44(4):384-394.

[6] 凌媛,王永,王淑贤,等. 生物标志物在海洋和湖泊古生态系统和生产力重建中的应用[J]. 地学前缘, 2022, 29(2):327-342.
Ling Y, Wang Y, Wang S X, et al. Application of biomarkers in reconstructing marine and lacustrine paleoecosystems and paleoproductivity: A review[J]. Earth Science Frontiers, 2022, 29(2):327-342.

[7] Goñi M A, Montgomery S. Alkaline CuO oxidation with a microwave digestion system: Lignin analyses of geochemical samples[J]. Analytical Chemistry, 2000, 72(14):3116-3121.

[8] Klein K, Gross-Schmölders M, Alewell C, et al. Chapter three-heating up a cold case: Applications of analytical pyrolysis GC/MS to assess molecular biomarkers in peat[M]//Advances in Agronomy. Academic Press, 2021: 115-159.

[9] Tsutsuki K, Esaki I, Kuwatsuka S. CuO-oxidation products of peat as a key to the analysis of the paleo-environmental changes in a wetland[J]. Soil Science and Plant Nutrition, 1994, 40(1):107-116.

[10] Meuzelaar H L C, Haider K, Nagar B R, et al. Comparative studies of pyrolysis-mass spectra of melanins, model phenolic polymers, and humic acids[J]. Geoderma, 1977, 17(3):239-252.

[11] Bracewell J M, Robertson G W, Williams B L. Pyrolysis-mass spectrometry studies of humification in a peat and a peaty podzol[J]. Journal of Analytical & Applied Pyrolysis, 1980, 2(1):53-62.

[12] Page D W. Characterisation of organic matter in sediment from Corin Reservoir, Australia[J]. Journal of Analytical and Applied Pyrolysis, 2003, 70(2):169-183.

[13] Kumar M, Boski T, Lima-Filho F P, et al. Environmental changes recorded in the Holocene sedimentary infill of a

tropical estuary[J]. Quaternary International, 2018, 476: 34-45.

[14] Saiz-Jimenez C, de Leeuw J W. Lignin pyrolysis products: Their structures and their significance as biomarkers [J]. Organic Geochemistry, 1986, 10(4-6): 869-876.

[15] Tinoco P, Almendros G, Gonzalez-Vila F J. Impact of the vegetation on the lignin pyrolytic signature of soil humic acids from Mediterranean soils[J]. Journal of Analytical and Applied Pyrolysis, 2002, 64(2): 407-420.

[16] Carr A S, Boom A, Chase B M, et al. Molecular fingerprinting of wetland organic matter using pyrolysis-GC/MS: An example from the southern cape coastline of South Africa [J]. Journal of Paleolimnology, 2010, 44(4): 947-961.

[17] Ohra-Aho T, Tenkanen M, Tamminen T. Direct analysis of lignin and lignin-like components from softwood kraft pulp by Py-GC/MS techniques[J]. Journal of Analytical and Applied Pyrolysis, 2005, 74(1-2): 123-128.

[18] van der Kaaden A, Boon J J, Haverkamp J. The analytical pyrolysis of carbohydrates. 2—Differentiation of homopolyhexoses according to their linkage type, by pyrolysis-mass spectrometry and pyrolysis-gas chromatography/mass spectrometry[J]. Biomedical Mass Spectrometry, 1984, 11(9): 486-492.

[19] Ninnes S, Tolu J, Meyer-Jacob C, et al. Investigating molecular changes in organic matter composition in two Holocene lake—Sediment records from central Sweden using pyrolysis-GC/MS[J]. Journal of Geophysical Research: Biogeosciences, 2017, 122(6): 1423-1438.

[20] Melenevskii V, Leonova G, Bobrov V, et al. Transformation of organic matter in the Holocene sediments of Lake Ochki (South Baikal region): Evidence from pyrolysis data[J]. Geochemistry International, 2015, 53(10): 903-921.

[21] Carr A S, Boom A, Chase B M, et al. Holocene sea level and environmental change on the west coast of South Africa: Evidence from plant biomarkers, stable isotopes and pollen[J]. Journal of Paleolimnology, 2015, 53(4): 415-432.

[22] Tolu J, Gerber L, Boily J F, et al. High-throughput characterization of sediment organic matter by pyrolysis-gas chromatography/mass spectrometry and multivariate curve resolution: A promising analytical tool in (paleo) limnology[J]. Analytica Chimica Acta, 2015, 880: 93-102.

[23] Xie M M, Sun Q, Dong H W, et al. *n*-Alkanes and compound carbon isotope records from Lake Yiheshariwusu in the Hulun Buir sandy land, northeastern China[J]. The Holocene, 2020, 30(10): 1451-1461.

[24] Schellekens J, Buurman P. *n*-Alkane distributions as palaeoclimatic proxies in ombrotrophic peat: The role of decomposition and dominant vegetation[J]. Geoderma, 2011, 164(3-4): 112-121.

[25] Shang W Y, Wang S X, Ling Y, et al. Holocene pyrolytic nitrogen compounds by using pyrolysis-GC/MS and its paleoclimatic implication from Jinchuan peatbog, NE China [J]. Quaternary International, 2022, 616: 109-119.

[26] Kebelmann K, Hornung A, Karsten U, et al. Intermediate pyrolysis and product identification by TGA and Py-GC/MS of green microalgae and their extracted protein and lipid components[J]. Biomass and Bioenergy, 2013, 49: 38-48.

[27] Lara-Gonzalo A, Kruge M A, Lores I, et al. Pyrolysis GC-MS for the rapid environmental forensic screening of contaminated brownfield soil[J]. Organic Geochemistry, 2015, 87: 9-20.

[28] Moldoveanu S C. Pyrolysis GC/MS, present and future (recent past and present needs)[J]. Journal of Microcolumn Separations, 2001, 13: 102-125.

[29] Schellekens J, Bradley J A, Kuyper T W, et al. The use of plant-specific pyrolysis products as biomarkers in peat deposits[J]. Quaternary Science Reviews, 2015, 123: 254-264.

[30] Gupta N S. Molecular preservation of Eurypterids[M]// Biopolymers: A molecular paleontology approach. Dordrecht: Springer Netherlands, 2014: 119-134.

[31] Lu X, Ma S, Chen Y, et al. Squalene found in alpine grassland soils under a harsh environment in the Tibetan Plateau, China[J]. Biomolecules, 2018, 8(4): 154-166.

[32] Piñeiro-Juncal N, Kaal J, Moreira J C F, et al. Cover loss in a seagrass Posidonia oceanica meadow accelerates soil organic matter turnover and alters soil prokaryotic communities[J]. Organic Geochemistry, 2021, 151: 104-140.

[33] Zhang Z, Wang J J, Lyu X, et al. Impacts of land use change on soil organic matter chemistry in the Everglades, Florida—A characterization with pyrolysis-gas chromatography-mass spectrometry[J]. Geoderma, 2019, 338: 393-400.

[34] Zhu R, Versteegh G J M, Hinrichs K U. Detection of microbial biomass in subseafloor sediment by pyrolysis-GC/MS[J]. Journal of Analytical and Applied Pyrolysis, 2016, 118: 175-180.

[35] Zúñiga D, Kaal J, Villacieros-Robineau N, et al. Tracing sinking organic matter sources in the NW Iberian upwelling system (NE Atlantic Ocean): Comparison between elemental, isotopic and molecular indicators [J]. Journal of Analytical and Applied Pyrolysis, 2019,

139:114-122.

[36] 尚文郁,孙静轶,谢曼曼,等.基于 Py-GC/MS 的沙漠湖泊直链脂肪族化合物分析及古气候应用初探[J].岩矿测试,2022,41(5):836-848.

Shang W Y, Sun J Y, Xie M M, et al. Py-GC/MS analysis method for aliphatic biomarker in desert lake sediment and its application in paleoclimatic study[J]. Rock and Mineral Analysis,2022,41(5):836-848.

[37] 丛浦珠,苏克曼.分析化学手册:质谱分析(第九分册)[M].北京:化学工业出版社,2000.

Cong P Z, Su K M. Handbook of analytical chemistry: Mass spectrometry (Chapter 9)[M]. Beijing: Chemical Industry Press,2000.

[38] Zhang J, Liu J, Liu R L. Effects of pyrolysis temperature and heating time on biochar obtained from the pyrolysis of straw and lignosulfonate[J]. Bioresource Technology, 2015,176:288-291.

[39] Garcia-Perez M, Wang X S, Shen J, et al. Fast pyrolysis of Oil Mallee Woody biomass: Effect of temperature on the yield and quality of pyrolysis products[J]. Industrial & Engineering Chemistry Research, 2008, 47(6): 1846-1854.

[40] Zhang H, Liao W, Zhou X, et al. Coeffect of pyrolysis temperature and potassium phosphate impregnation on characteristics, stability, and adsorption mechanism of phosphorus-enriched biochar[J]. Bioresource Technology,2022,344:126273.

[41] Singh B P, Cowie A L, Smernik R J. Biochar carbon stability in a clayey soil as a function of feedstock and pyrolysis temperature[J]. Environmental Science & Technology,2012,46(21):11770-11778.

[42] Cui D, Li J, Zhang X, et al. Pyrolysis temperature effect on compositions of basic nitrogen species in Huadian shale oil using positive-ion ESI FT-ICR MS and GC-NCD[J]. Journal of Analytical and Applied Pyrolysis, 2021,153:104980.

[43] Kruge M A, Permanyer A. Application of pyrolysis-GC/MS for rapid assessment of organic contamination in sediments from Barcelona harbor[J]. Organic Geochemistry,2004,35(11):1395-1408.

[44] Kaal J, Cortizas A M, Rydberg J, et al. Seasonal changes in molecular composition of organic matter in lake sediment trap material from Nylandssjön, Sweden[J]. Organic Geochemistry,2015,83-84:253-262.

[45] Fabbri D, Sangiorgi F, Vassura I. Pyrolysis-GC-MS to trace terrigenous organic matter in marine sediments: A comparison between pyrolytic and lipid markers in the Adriatic Sea[J]. Analytica Chimica Acta, 2005, 530(2):253-261.

[46] Sigleo A C, Hoering T C, Helz G R. Composition of estuarine colloidal material: Organic components[J]. Geochimica et Cosmochimica Acta, 1982, 46(9): 1619-1626.

[47] Kaal J. Analytical pyrolysis in marine environments revisited[J]. Analytical Pyrolysis Letters,2019.

[48] Kaal J, Lavery P S, Martínez Cortizas A, et al. Reconstruction of 7500 years of coastal environmental change impacting seagrass ecosystem dynamics in Oyster Harbour (SW Australia)[J]. Palaeogeography, Palaeoclimatology, Palaeoecology,2020,558:109953.

[49] Kaal J, Martinez Cortizas A, Mateo M A, et al. Deciphering organic matter sources and ecological shifts in blue carbon ecosystems based on molecular fingerprinting[J]. Science of the Total Environment, 2020, 742: 140554.

[50] Boateng A A, Hicks K B, Vogel K P. Pyrolysis of switchgrass (Panicum virgatum) harvested at several stages of maturity[J]. Journal of Analytical & Applied Pyrolysis, 2006,75(2):55-64.

[51] Faure P, Jeanneau L, Lannuzel F. Analysis of organic matter by flash pyrolysis-gas chromatography-mass spectrometry in the presence of Na-smectite: When clay minerals lead to identical molecular signature[J]. Organic Geochemistry,2006,37(12):1900-1912.

[52] Zhang J, Wu C, Hou W, et al. Biological calcium carbonate with a unique organic-inorganic composite structure to enhance biochar stability[J]. Environmental Science: Processes & Impacts,2021,23(11):1747-1758.

[53] Chmiel H E, Niggemann J, Kokic J, et al. Uncoupled organic matter burial and quality in boreal lake sediments over the Holocene[J]. Journal of Geophysical Research: Biogeosciences,2015,120(9):1751-1763.

[54] Moingt M, Lucotte M, Paquet S, et al. Deciphering the impact of land-uses on terrestrial organic matter and mercury inputs to large boreal lakes of central Québec using lignin biomarkers[J]. Applied Geochemistry, 2014,41:34-48.

[55] Opsahl S, Benner R. Early diagenesis of vascular plant tissues: Lignin and cutin decomposition and biogeochemical implications[J]. Geochimica et Cosmochimica Acta,1995,59(23):4889-4904.

[56] Dittmar T, Lara R J. Molecular evidence for lignin degradation in sulfate-reducing mangrove sediments (Amazônia, Brazil)[J]. Geochimica et Cosmochimica Acta,2001,65(9):1417-1428.

[57] Sanjurjo-Sánchez J, Kaal J, Fenollós J L M. Organic matter from bevelled rim bowls of the middle Euphrates: Results from molecular characterization using pyrolysis-GC-MS[J]. Microchemical Journal,2018,141:1-6.

[58] Kaal J, Cortizas A M, Biester H. Downstream changes in

molecular composition of DOM along a headwater stream in the Harz Mountains (central Germany) as determined by FTIR, pyrolysis-GC-MS and THM-GC-MS[J]. Journal of Analytical and Applied Pyrolysis, 2017, 126: 50-61.

[59] 杨丽阳,吴莹,黄俊华,等. 大九湖泥炭柱样的木质素特征[J]. 地球化学,2009,38(2):133-139.
Yang L Y, Wu Y, Huang J H, et al. Lignin characteristics in a peat core of Lake Dajiu[J]. Geochimica, 2009, 38(2):133-139.

[60] 刘月,王敏,张婷,等. 杭州湾外泥质区柱状沉积物中木质素的分布特征及其环境指示意义[J]. 海洋环境科学,2017,36(1):8-14.
Liu Y, Wang M, Zhang T, et al. Distribution characteristics of lignin in sediment cores from the mud area off Hangzhou Bay and the implication for regional sedimentary environment[J]. Chinese Journal of Marine Environmental Science, 2017, 36(1):8-14.

[61] Tuomela M, Hatakka A. Oxidative fungal enzymes for bioremediation[M]//Comprehensive biotechnology (The second edition). Burlington: Academic Press, 2011.

[62] Otsuka Y, Sonoki T, Ikeda S, et al. Detection and characterization of a novel extracellular fungal enzyme that catalyzes the specific and hydrolytic cleavage of lignin guaiacylglycerol $\beta$-aryl ether linkages[J]. European Journal of Biochemistry, 2003, 270(11): 2353-2362.

[63] Wong D W S. Structure and action mechanism of ligninolytic enzymes[J]. Applied Biochemistry and Biotechnology, 2009, 157(2):174-209.

[64] Boerjan W, Ralph J, Baucher M. Lignin Biosynthesis[J]. Annual Review of Plant Biology, 2003, 54(1):519-546.

[65] Philben M, Ziegler S E, Edwards K A, et al. Soil organic nitrogen cycling increases with temperature and precipitation along a boreal forest latitudinal transect[J]. Biogeochemistry, 2016, 127(2):397-410.

[66] Hawkes C V, Kivlin S N, Rocca J D, et al. Fungal community responses to precipitation[J]. Global Change Biology, 2015, 17(4):1637-1645.

[67] Xiao J, Chang Z, Wen R, et al. Holocene weak monsoon intervals indicated by low lake levels at Hulun Lake in the monsoonal margin region of northeastern Inner Mongolia, China[J]. Holocene, 2009, 19(6):899-908.

[68] Wen R, Xiao J, Chang Z, et al. Holocene precipitation and temperature variations in the East Asian monsoonal margin from pollen data from Hulun Lake in northeastern Inner Mongolia, China[J]. Boreas, 2010, 39(2): 262-272.

[69] 曾琳,鹿化煜,弋双文,等. 末次盛冰期和全新世大暖期呼伦贝尔沙地的环境变化[J]. 第四纪研究,2013,33(2):243-251.
Lin Z, Lu H Y, Yi S W, et al. Environmental changes of Hulun Buir dunefield in northeastern China during the last Glacial maximum and Holocene optimum[J]. Quaternary Sciences, 2013, 33(2):243-251.

[70] Li S H, Sun J. Optical dating of Holocene dune sands from the Hulun Buir Desert, northeastern China[J]. Holocene, 2006, 16(3):457-462.

[71] 温锐林,肖举乐,常志刚,等. 全新世呼伦湖区植被和气候变化的孢粉记录[J]. 第四纪研究,2010,30(6): 1105-1115.
Wen R L, Xiao J L, Chang Z G, et al. Holocene vegetation and climate changes reflected by the pollen record of Hulun Lake, north eastern Inner Mongolia[J]. Quaternary Sciences, 2010, 30(6):1105-1115.

[72] Na L, Yu L, Guang B, et al. Drought reconstruction in eastern Hulun Buir steppe, China and its linkages to the sea surface temperatures in the Pacific Ocean[J]. Journal of Asian Earth Sciences, 2016, 115:298-307.

[73] 张风菊,薛滨,姚书春. 中全新世以来呼伦湖沉积物碳埋藏及其影响因素分析[J]. 湖泊科学,2018,30(1):234-244.
Zhang F J, Xue B, Yao S C. Organic carbon burial and its driving mechanism in the sediment of Lake Hulun, northeastern Inner Mongolia, since the mid-Holocene[J]. Journal of Lake Sciences, 2018, 30(1):234-244.

[74] 董浩伟,赵佳玉,曾凡刚,等. 柱色谱分离-分子筛络合洗脱过程中正构烷烃单体碳同位素分馏研究[J]. 岩矿测试,2021,40(3):349-357.
Dong H W, Zhao J Y, Zeng F G, et al. Study on specific carbon isotope fractionation of *n*-alkanes during column chromatography separation-molecular sieve complexation adsorption[J]. Rock and Mineral Analysis, 2021, 40(3):349-357.

[75] 王宁,朱庆增,谢曼曼,等. 尿素络合法分离-气相色谱/同位素质谱法分析土壤和植物中低含量(ppm级)正构烷烃的碳同位素[J]. 岩矿测试,2015,34(4):471-479.
Wang N, Zhu Q Z, Xie M M, et al. An improved urea adduction method for analyzing carbon isotope of ppm-level *n*-alkanes in soil and plant samples[J]. Rock and Mineral Analysis, 2015, 34(4):471-479.

[76] Routson C C, McKay N P, Kaufman D S, et al. Mid-latitude net precipitation decreased with Arctic warming during the Holocene[J]. Nature, 2019, 568(7750): 83-87.